Crystal Structure of Form I of Syndiotactic Polypropylene

Claudio De Rosa,* Finizia Auriemma, and Paolo Corradini

Dipartimento di Chimica Università di Napoli Federico II, Via Mezzocannone 4, 80134 Napoli, Italy

Received January 29, 1996; Revised Manuscript Received June 21, 1996[⊗]

ABSTRACT: The crystal structure of the stable crystalline form of syndiotactic polypropylene (s-PP) may be taken, only as a first approximation, as body-centered orthorhombic and described in the space group *Ibca* (in which the chains maintain their full, ideal 2_122 symmetry). Indeed, the splitting of the resonance of the methyl carbons, observed in the solid state ^{13}C NMR spectra of annealed samples of s-PP in this crystalline form, reported by Sozzani et al., and the observation by Lovinger and Lotz of a 011 reflection in the electron diffraction spectra of single crystals of s-PP grown at high temperature may be taken as indications of a symmetry lower than that of *Ibca* for the limit, fully ordered structure. We have refined, through the Rietveld method, various structural models for which right- and left-handed helices are repeated along the *a* and *b* axes as in the space group *Ibca*, but the full 2_122 chain symmetry is not maintained. We started with the model of higher symmetry (space group *Ibca*) and then space groups of lower symmetry were analyzed. In the refined models, while the unit cell constants are almost unvaried ($a = 14.31 \pm 0.07$ Å, $b = 11.15 \pm 0.02$ Å, $c = 7.5 \pm 0.1$, $\gamma = 90.3 \pm 1.5°$) and, thus, the positions of the chain axes are practically the same as in the *Ibca* space group, the lattice is primitive (*P*), instead of body-centered (*I*), and the chains are slightly rotated (±5°) around the chain axis and significantly shifted (≈0.07*c*) along the chain axis with respect to the previously assumed position, having 2_122 crystallographic symmetry. This results in a noncrystallographic equivalence of the methyl groups, which have then slightly different packing environments. The space group is $P2_1/a$.

Introduction

Syndiotactic polypropylene (s-PP) was synthesized for the first time by Natta et al.[1] The resulting polymer had a stereoblock structure with almost syndiotactic sequences prevailing in respect to isotactic ones and head-to-head/tail-to-tail regioirregular defects.[2,3] As a consequence of the poor syndiospecificity of the vanadium-based catalysts and of the scarcely interesting physico-chemical properties of the polymer, syndiotactic polypropylene has received in the past only very little attention.

Highly stereoregular and regioregular syndiotactic polypropylene has been synthesized only recently with new metallocene homogeneous catalysts;[4] the properties of this new syndiotactic polypropylene have been greatly improved and this has focused the interest of the research on s-PP, resulting in numerous studies aimed at elucidating the structure and the polymorphism of s-PP.[5−19]

The polymorphic behavior of s-PP has been known for many years;[20−22] a stable modification, characterized by chains in the s(2/1)2 helical conformation packed in an orthorhombic lattice,[20,21] and an unstable form, characterized by *trans* planar chains,[22] have been described in the past. The recent structural studies on s-PP based on electron diffraction,[5−8] X-ray diffraction,[9,11,12,16,17] and solid state ^{13}C NMR spectroscopy[18,19] have shown that the polymorphism of s-PP is more complex for the presence of new crystalline modifications as well as for the presence of different amounts of disorder in the crystalline phases depending on the degree of stereoregularity and the mechanical and thermal history of the samples. In order to clarify the description of the polymorphism of s-PP, we suggest a nomenclature for the various limiting ordered crystalline forms.

Form I is the stable form obtained under the most common conditions of crystallization (melt and solution crystallization) in powder samples and single crystals of s-PP. This form, found by Lovinger, Lotz, et al.,[5−8] is characterized by chains in the s(2/1)2 helical conformation packed in an orthorhombic unit cell with axes $a = 14.5$ Å, $b = 11.2$ Å, and $c = 7.4$ Å shown in Figure 1A. The axes of the helices are in the positions (0, 0, *z*) and ($^1/_2$, 0, *z*) of the unit cell and the main X-ray peaks in the powder spectrum are at $d = 7.25$, 5.6, 4.70, and 4.31 Å ($2\theta = 12.2$, 15.8, 18.8, and 20.6°, Cu Kα). In the ideal limit-ordered structure of form I right-handed and left-handed helices alternate along *a* and *b* axes (Figure 1A) (as imposed by the presence of the (211) reflection at $d = 4.70$ Å); the space group proposed was *Ibca*.[5,8]

Single crystals of s-PP grown at low temperatures (<130 °C), powder samples rapidly precipitated from solution, and samples crystallized by quenching the melt present a departure from the ideal fully antichiral body-centered packing of Figure 1A, as revealed by the weakness or, in same cases, by the absence of the (211) reflection at $d = 4.70$ Å in the electron and X-ray diffraction patterns.[5,8,9] For these samples the structure may be represented by a unit cell with axes $a = 14.5$ Å, $b = 5.60$ Å, and $c = 7.4$ Å (Figure 1B) with antichiral packing of chains only along the *a* axis; the space group proposed was *Pcaa*.[5,9]

Form II is obtained in annealed fiber samples of s-PP (often in a mixture with form I). It corresponds to the C-centered structure deduced by Corradini et al.[20,21] from the X-ray diffraction fiber spectra of drawn fibers of s-PP samples available in 1967, which is shown in Figure 1C. This form is characterized by chains in the s(2/1)2 helical conformation packed in the orthorhombic unit cell with axes $a = 14.5$ Å, $b = 5.60$ Å, and $c = 7.4$ Å. The axes of the helices are in the positions (0, 0, *z*) and ($^1/_2$, $^1/_2$, *z*) of the unit cell, and the main X-ray peaks in the powder spectrum are at $d = 7.25$, 5.22, and 4.31 Å ($2\theta = 12.2$, 17.0, and 20.6°, Cu Kα).[9,21]. The space group proposed for the limit ordered structure of form II was $C222_1$,[21] for which helices of the same chirality are included in the unit cell (Figure 1C).

Also for form II, the space group $C222_1$ corresponds to a limit-ordered modification; disorder corresponding to statistical substitution of right- and left-handed helices in the lattice positions could be present.[9,11]

[⊗] Abstract published in *Advance ACS Abstracts,* September 1, 1996.

S0024-9297(96)00132-5 CCC: $12.00

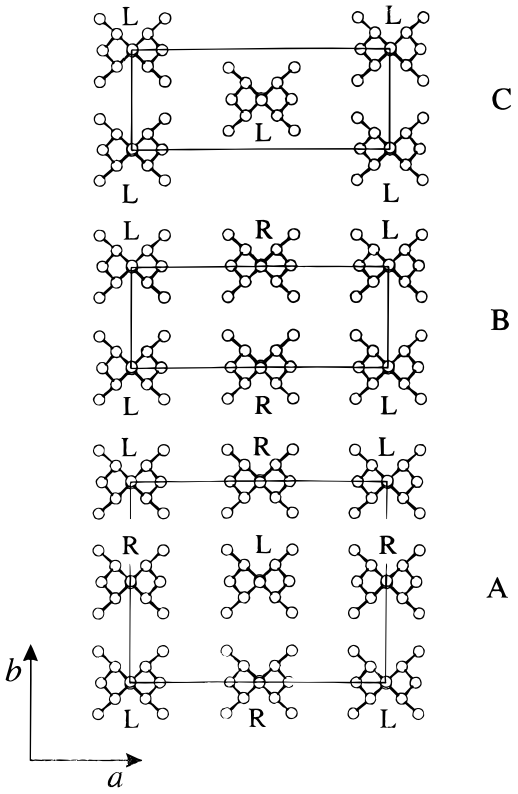

Figure 1. Models of packing of limit orthorhombic modifications of s−PP: (A) space group *Ibca*; (B) space group *Pcaa*; (C) space group $C222_1$. R = right handed, L = left handed.

Form III is obtained by stretching at room temperature compression-moulded samples of s-PP, as found by Natta et al.,[22] and is characterized by chains in zigzag *trans* planar conformation.[22] The crystal structure of form III has been reported recently by Chatani et al.;[16] *trans* planar chains are packed in an orthorhombic unit cell with axes $a = 5.22$ Å, $b = 11.17$ Å, and $c = 5.06$ Å; the space group proposed is $P2_1cn$.[16] When the fiber samples of form III are annealed above 100 °C (under the condition of fixed length), the *trans* planar form transforms completely into the two-fold helical form; a fiber with a mixture of crystals of form I and form II is generally obtained.[9]

Form IV was obtained by Chatani et al.[17] by exposing fiber specimens in the zigzag *trans* planar form (form III) to organic solvents (e.g. benzene at temperatures below 50 °C).[17] It is characterized by helices in a $(T_6G_2T_2G_2)_n$ conformation, packed in a triclinic unit cell with axes $a = 5.72$ Å, $b = 7.64$ Å, and $c = 11.6$ Å and $\alpha = 73.1°$, $\beta = 88.8°$, and $\gamma = 112.0°$.[17] Form IV is transformed readily into the two-fold helical forms by annealing above 50 °C.

The polymorphism of s-PP is complicated by the fact that, depending on the degree of stereoregularity and the mechanical and thermal history of the samples, s-PP shows different amounts of statistical disorder in the crystalline packing.[5−9,11,12] Broad peaks observed in the X-ray powder and fiber diffraction spectra,[9] streaks observed in the electron diffraction spectra,[5−8] and extra resonances observed in the solid state ^{13}C NMR spectra[18,19] have been explained through models characterized by disorder in the packing[11,12] and in the conformation of the chains.[18] In particular the proposed models are characterized by (a) departure from the regular alternation of two-fold helices of opposite chirality along the *a* and *b* axes in the case of form I;[9,11,12] (b) departure from the fully isochiral packing of two-fold helices in the case of form II;[9,11,12] (c) a statistical mixture of crystals of form I and form II[9,11,12] (this kind of disorder has been observed in single crystals of s-PP obtained at low temperatures,[7,8] as well as in fiber and powder specimens of s-PP[9,11,12]); (d) conformational disorder, in the case of samples of s-PP quench-precipitated from solutions, characterized by the presence of *trans* planar portions of chains connecting portions in s(2/1)2 helical conformations.[18] In the resulting structure the chains would be packed according to an orthorhombic lattice centered on the C face: for the ordered regions like in form II, for the region comprising the defects like in form IV[18].

In this paper the crystal structure of form I is analyzed in detail. Indeed, the presence, in the electron diffraction spectra of single crystals of s-PP grown at high temperature,[8] of the (011) reflection (not permitted by the space group *Ibca*) indicates that the limit-ordered structure of form I can be described only approximately by the space group *Ibca*. Moreover the splitting of the resonance of the methyl carbons observed in the solid state ^{13}C NMR spectra of annealed samples of s-PP in form I, reported by Sozzani et al.,[15] indicates that the space group *Ibca*, for which the methyl carbons are all equivalent, is not fully correct. As already suggested in ref 9 the mode of packing of the chains in form I could be very similar to that of Figure 1A but in a space group of lower symmetry. In this paper a refinement of the structure of form I, performed with the Rietveld method, is presented.

Experimental Section

The s-PP sample was supplied by Montell.

The polymer was synthesized with syndiospecific homogeneous catalyst based on a column-4-metallocene (isopropylidene(cyclopentadienyl)(9-fluorenyl)zirconium dichloride)/methylaluminoxane system.[4] The sample ($MW = 260 \times 10^3$) is highly syndiotactic with 94.5% fully syndiotactic pentads (*rrrr*). The sample corresponds to sample A of ref 9.

A highly crystalline, ordered form I was obtained by isothermal crystallization from the melt. The sample was kept for 5 min at ≈200 °C in a N_2 atmosphere (melting point, 153 °C); it was then rapidly cooled to 140 °C and kept at this temperature for 14 h.

X-ray powder diffraction spectra were recorded at room temperature with an automatic Philips diffractometer using Ni-filtered Cu Kα radiation and a step scan procedure. The range of 2θ diffraction angle examined was 5−55°, the count time for each step was equal to 60 s/step, and the step was 0.04° (2θ).

The refinement procedure was done through the use of the program DEBVIN first developed by Immirzi[23] and hence revised and implemented by Bruckner.[24−26]

Method of Refinement

The refinement was performed with the full profile X-ray powder diffraction refinement procedure (Rietveld method), using the same approach employed in the case of the crystal structure refinement of other polymers.[24−27]

For the crystalline structure of polymers, it is possible to refine, with this method, all together the chain conformation, the packing parameters, the cell constants, and nonstructural parameters.

The minimized function is

$$F = \sum W_i(I_{ci} - I_{oi})^2 + \sum u_j(G_{oj} - G_j)^2$$

with I_{oi} and I_{ci} the observed and the calculated values of the intensity profile at the diffraction angle $2\theta_i$ and

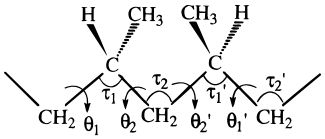

Figure 2. Portion of the chain of sPP. The definition of the torsion and bond angles are indicated.

Table 1. Refined Fractional Coordinates of the Carbon Atoms of the Asymmetric Unit for the Models Corresponding to the Space Groups *Ibca*, *Pbca*, and *P*2$_1$/*a*[a]

	x/*a*	*y*/*b*	*z*/*c*	occupation factor
		Ibca		
1-CH_2 (GT·TG)	0.2500(0)	−0.005(1)	0.0000(0)	0.5
2-CH	0.3106(4)	−0.0809(6)	0.1238(4)	1
3-CH_2 (TG· GT)	0.3658(1)	0.0000(0)	0.2500(2)	0.5
4-CH_3	0.3770(7)	−0.1564(5)	0.0106(8)	1
		Pbca		
1-CH_2 (GT· TG)	0.2539(8)	−0.0040(3)	−0.067(1)	
2-CH	0.308(1)	−0.0867(6)	0.058(1)	
3-CH_2 (TG·GT)	0.368(1)	−0.014(1)	0.188(2)	
4-CH_3	0.370(1)	−0.171(1)	−0.052(2)	
5-CH	0.313(2)	0.0707(9)	0.309(1)	
6-CH_3	0.380(2)	0.151(1)	0.413(2)	
		*P*2$_1$/*a*		
1-CH_2 (GT·TG)	0.249(1)	−0.004(1)	−0.032(2)	
2-CH	0.307(2)	−0.088(2)	0.084(2)	
3-CH_2 (TG·GT)	0.370(2)	−0.016(3)	0.209(3)	
4-CH_3	0.366(2)	−0.171(2)	−0.032(4)	
5-CH	0.318(2)	0.066(3)	0.338(2)	
6-CH_3	0.387(3)	0.145(4)	0.439(2)	
1′-CH_2 (GT·TG)	0.760(1)	0.504(1)	0.112(3)	
2′-CH	0.811(2)	0.581(3)	0.974(4)	
3′-CH_2 (TG·GT)	0.869(2)	0.512(3)	0.837(4)	
4′-CH_3	0.872(4)	0.676(4)	1.065(4)	
5′-CH	0.812(2)	0.426(2)	0.719(3)	
6′-CH_3	0.877(2)	0.357(3)	0.595(4)	

[a] For the space group *P*2$_1$/*a* the asymmetric unit corresponds to two independent structural units (two monomeric units) labeled in Figure 7. The occupation factors of the atoms in the asymmetric units of *Pbca* and *P*2$_1$/*a* space groups are all equal to 1.

W_i a weight factor which was placed equal to $W_i = 1/I_{oi}$; G_{oj} and G_j are the values which a given geometrical variable (i.e., bond lengths, bond angles, dihedral angles, distances between nonbonded atoms, etc.) is desired to assume and the corresponding value assumed by that variable at the given point of the refinement procedure, respectively. To introduce these constraining conditions, Lagrangian's undetermined multipliers u_j are employed.[28]

In carrying out the structural refinement with the present approach, the agreement factor R_2' is defined as:

$$R_2' = \sum |I_{oi} - I_{ci}| / \sum I_{ni}$$

with $I_{ni} = I_{oi} - I_{bi}$ where I_{bi} is the background intensity which includes the amorphous contribution. The amorphous diffraction profile has been included by recording the X-ray powder diffraction pattern of an atactic polypropylene sample suitably prepared.

In Figure 2 a portion of the chain of s-PP is shown with the definition of the torsion angles θ_1, θ_2, θ_1', and θ_2' and bond angles τ_1, τ_2, τ_1', and τ_2'.

An asymmetric unit composed of one, two, or four monomeric units, depending on the space group, as we shall see, was generated. We refined the orientation of the asymmetric unit relative to the axes *x*, *y*, and *z*, so that the torsion angles θ_1 and θ_2 resulted simply by the symmetry relations connecting the successive monomeric units. The C−C bond lengths were kept constant during the refinement procedure and equal to 1.53 Å.

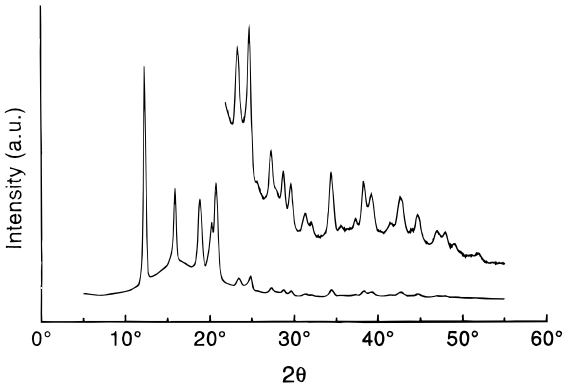

Figure 3. X-ray powder diffraction spectrum of form I of s-PP obtained by isothermal crystallization from the melt at 140 °C for 14 h. The diffraction profile for $2\theta > 22°$ on an enlarged intensity scale is also reported.

The cell constants, *a*, *b*, and *c*, were of course refined.

Some nonstructural parameters were refined. In particular, it was necessary to refine the scaling factor for the amorphous X-ray powder diffraction profile, in order to put the latter profile on the same intensity scale of the spectrum of the semicrystalline polymer. An additional baseline (assumed to be a straight line) spanning the whole spectrum, with nodes having abscissa $2\theta = 4$ and 50° and the ordinate to be refined on the intensity scale, was considered.

The peak shape was assumed to be a Cauchy function with half-height width *H* equal to

$$H = (U \tan^2[\theta] + V \tan[\theta] + W)^{1/2}$$

with θ the diffraction angle, *U* and *V* two variables to be optimized, and *W* depending on the (*hkl*) values through an adjustable estimation of average crystallite dimensions L_a, L_b, and L_c along the axes of the unit cell *a*, *b*, and *c*, respectively.[24,29,30]

We recall that the refined values of L_a, L_b, and L_c do not give immediately the real average crystalline dimensions since the instrumental broadening is present and affects the peak shape; therefore, further elaboration would be required to obtain physically more meaningful data.

Also, a factor relative to the asymmetry of the diffraction peaks was refined. This peak asymmetry was described by adopting two half-peak functions with different half-height widths H' and H'' with $H' - H'' = 2HA/(2\theta)^2$, with *H* the half-height width without asymmetry and *A* a parameter to be refined.

A zero-point correction (zero shift) of the experimental 2θ scale was evaluated.

The thermal parameters (assumed isotropic) of all the atoms were always kept constant at a value of 8 Å^2.

Results and Discussion

The X-ray powder diffraction pattern of s-PP, crystallized from the melt at 140 °C for 14 h, is reported in Figure 3. The presence of a reflection at $d = 5.60$ Å ($2\theta = 15.8°$, Cu Kα) and of the reflection at $d = 4.70$ Å ($2\theta = 18.8°$, Cu Kα) and the absence of the reflection at $d = 5.22$ Å ($2\theta = 17.0°$, Cu Kα) indicate that this sample is in a well-crystallized and ordered form I (Figure 1A).

We have refined various structural models all having the same main feature, that is right-handed and left handed-helices alternating along *a* and *b* axes as in Figure 1A. We started with the model of higher

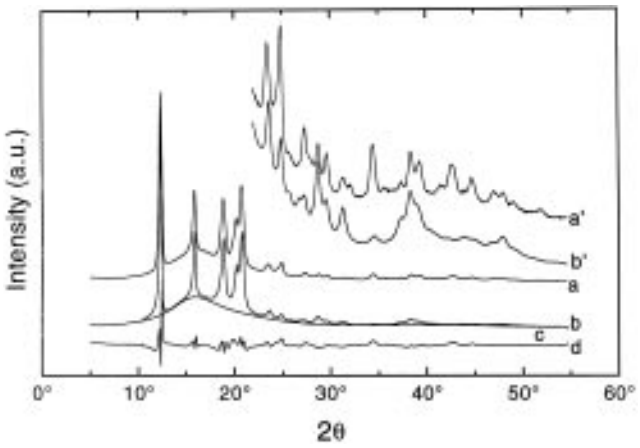

Figure 4. Comparison between the observed (curve a) and calculated, for the space group *Ibca* (curve b), X-ray powder diffraction profiles of form I of s-PP. The X-ray profile of the amorphous sample suitably scaled (curve c) and the difference between observed and calculated profiles (curve d) are also shown. The experimental (curve a′) and calculated (curve b′) profiles for $2\theta > 22°$ on an enlarged intensity scale are also reported.

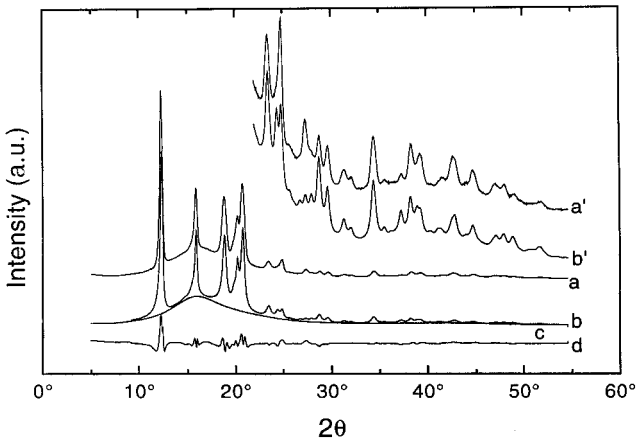

Figure 5. Comparison between the observed (curve a) and calculated, for the space group *Pbca* (curve b), X-ray powder diffraction profiles of form I of s-PP. The X-ray profile of the amorphous sample suitably scaled (curve c) and the difference between observed and calculated profiles (curve d) are also shown. The experimental (curve a′) and calculated (curve b′) profiles for $2\theta > 22°$ on an enlarged intensity scale are also reported.

symmetry (space group *Ibca*) and then space groups of lower symmetry were analyzed.

Preliminary structure factor calculations have shown that all these models present the same calculated intensity of the strong reflection at $d = 7.25$ Å ($2\theta = 12.2°$, Cu Kα), while differences are observable for the reflections at higher values of 2θ. For this reason the refinements have been performed with the weight factor $W_i = 0$ for $2\theta < 13°$.

The refinement for the space group *Ibca* gives an agreement factor $R_2' = 22\%$. In this model the coincidence of the crystallographic binary axes of the space group *Ibca* with those of the s(2/1)2 chain, prevents the chain from rotating around its axis and translating along *z*.

A comparison between the observed (curve a) and calculated (curve b) X-ray powder diffraction profiles for the space group *Ibca*, is reported in Figure 4. The X-ray profile of the amorphous sample suitably scaled (curve c) and the difference between observed and calculated profiles (curve d) are also shown in Figure 4.

Table 2. Refined Values of the Structural Parameters for Form I of s−PP[a]

	space group		
	Ibca	*Pbca*	$P2_1/a$ (*c*, unique axis)
a (Å)	14.33(6)	14.32(7)	14.31(7)
b (Å)	11.15(3)	11.15(3)	11.15(2)
c (Å)	7.5(1)	7.5(1)	7.5(1)
γ (deg)			90.3(1.5)
R_2' (%)	22	13.3	11.6
Asymmetric Unit			
	space group		
			$P2_1/a$ (*c*, unique axis)
	Ibca	*Pbca*	unprimed chain[b] / primed chain[b]
ϑ_1 (deg)	61.0	62.8	61.3 / 61.8
ϑ_1' (deg)	61.0	61.8	60.9 / 61.8
ϑ_2 (deg)	−177.3	−175.8	−174.7 / 172.7
ϑ_2' (deg)	−177.3	178.6	−179.3 / −167.7
τ_1 (deg)	110.2	111.0	116.1 / 110.2
τ_2 (deg)	112.8	113.7	115.0 / 113.6
τ_1' (deg)	110.2	112.7	110.2 / 115.8
τ_2' (deg)	117.7	114.8	114.8 / 114.8
ω (deg)		5.3	5.8 / −4.4

[a] The numbers in parentheses represent the standard deviations. [b] See Figure 7.

Table 3. Refined Nonstructural Parameters[a]

space group	*Ibca*	*Pbca*	$P2_1/a$ (*c*, unique axis)
profile function parameters			
U (deg²)	7(1)	0	0
V (deg²)	−0.6(1)	0.46(5)	0.67(5)
average dimensions of the crystallites			
L_a (Å)	$2.1(3) \times 10^2$	$1.5(1) \times 10^2$	$2.0(1) \times 10^2$
L_b (Å)	$2.5(2) \times 10^2$	$2.5(1) \times 10^2$	$2.7(1) \times 10^2$
L_c (Å)	93(6)	91(3)	88(3)
asymmetry factor			
A (deg)	79(1)	54(6)	61(6) (deg²)

[a] The numbers in parentheses represent the standard deviations.

It is apparent from the inset in Figure 4, showing the experimental (curve a′) and calculated (curve b′) profiles for $2\theta > 22°$ on an enlarged intensity scale, that the most relevant differences between the observed and the calculated profiles are for high values of 2θ. Indeed, the X-ray diffraction pattern around the reflections at $2\theta = 24.8$, 27.2, 28.8, and 29.5° (curve a′) is not well reproduced in the calculations (curve b′), and the reflections at $2\theta = 34.3$, 42.5, and 44.6°, observed in the experimental curve a′, are almost absent in the calculated curve b′. The fractional coordinates of the asymmetric unit in the refined model are reported in Table 1. The values of the refined structural and nonstructural parameters are reported in Tables 2 and 3, respectively. This analysis, besides the predicted extinction, for the space group *Ibca*, of the (011) reflection, observed instead in some of the electron diffraction spectra,[8] indicates that the space group *Ibca* may describe the crystal structure of form I of s-PP, only in a first approximation.

Space groups with lower symmetry than *Ibca* can be obtained by successive eliminations of crystallographic symmetry elements. The elimination of the two-fold axes perpendicular to the chain axes leads to the space group *Pbca*. In this model, chains along the *a* and *b* axes are still related by glide planes and inversion centers but the chains are free to rotate around their

axes and to translate along *z*. The refinement for the space group *Pbca* leads to a unit cell with $a = 14.32$ Å, $b = 11.15$ Å, and $c = 7.5$ Å and gives an agreement factor $R_2' = 13.3\%$. A comparison between the observed (curves a and a′) and calculated (curves b, and b′) X-ray powder diffraction profiles is reported in Figure 5. A good agreement, also at high values of 2θ, is apparent. In particular, the reflections at $2\theta = 34.3$, 42.5, and 44.6° are now present also in the calculated profile (curve b′). The fractional coordinates of the asymmetric unit in the refined model are reported in Table 1. The values of the refined structural and nonstructural parameters are reported in Tables 2 and 3, respectively. In this refined model, the noncrystallographic binary axes perpendicular to the chain axis and crossing the methylene groups in the TG·GT conformational environment in the $a-b$ projection (where the dot indicates the position of the methylene group, T stands for *trans* and G for *gauche*) are rotated by an angle $|\omega| \approx 5°$ with respect to their original position in the *Ibca* space group. Also, the methylene groups placed in a GT·TG conformational environment are displaced now by $0.07c$ along *z* from the inversion center placed at heights 0 (or $^1/_2c$) (still, in the *Ibca* space group these methylene groups were at the same height as the inversion centers). As a consequence consecutive *bc* layers of chains along *a* are displaced by $0.14c$ along *z*, whereas the chains inside each *bc* layer are still related by a *c* glide plane perpendicular to *b*, like in the *Ibca* space group.

Some discrepancies with respect to the experimental data are, however, present also for the space group *Pbca*. First of all in the powder spectra of Figure 5 it is apparent that the intensities of the reflections at $2\theta = 24.8°$ and 27.2° are not well reproduced in the calculated profile (curve b′); moreover, the presence of the glide plane *b* perpendicular to the *a* axis of the unit cell still gives the systematic extinction of the (0*kl*) reflections with $k = 2n + 1$.

The agreement may be improved if the symmetry of the space group is lowered further. For instance, it is possible to remove the systematic extinction of (0*kl*) reflections with $k = 2n + 1$, upon elimination of the *b* crystallographic glide plane in the *Pbca* space group symmetry. The symmetry left leads to the $P2_1ca$ space group. More generally, any small distortion in the chain symmetry or in the packing could favor a better agreement with the experimental diffraction data. In practice, starting from this point, we could examine in cascade all the space groups of lower symmetry than *Pbca*, implying such distortions. We prefer to follow the indications of Lovinger, Lotz, et al. in ref 8, however. They suggest that the weak reflection (011) apparent in the electron diffraction patterns may arise from *c*-axis packing defects. For instance this reflection appears in the simulated electron diffraction spectra with intensity in reasonable agreement with the experiments, when one of the four chains in the unit cell is displaced by 10% of the length of the *c*-axis in the chain direction, as an example .[8] The same holds true also if two chains per unit cell, placed at 0 and *b*/2, are displaced by 5% of the *c* axis along the chain axis direction in opposite directions, as an example. As already noticed by Lovinger, Lotz, et al. in ref 8, not all the displacements lead to a satisfying agreement with the experimental data, however. The packing situation in the *Ibca* and *Pbca* space groups, in a projection perpendicular to the *a* axis, is shown in Figure 6A,B, respectively. The traces a (in phase) and b (out of phase) relative to the (011) crystallographic plane are indicated. It is evident that the displacement pattern of the chains along *c* is not enough to produce the observation of the (011) reflection; hence some other kind of displacement combinations in the relative shift along *c* of the chains should be introduced. In order to introduce those shift combinations crystallographically, we chose to eliminate the two glide planes from the space group *Pbca*, hence producing a change from the orthorhombic symmetry to a monoclinic symmetry. Restricting ourselves to those monoclinic space groups with an inversion center and allowing the s(2/1) chain symmetry to be preserved, we performed the following examination.

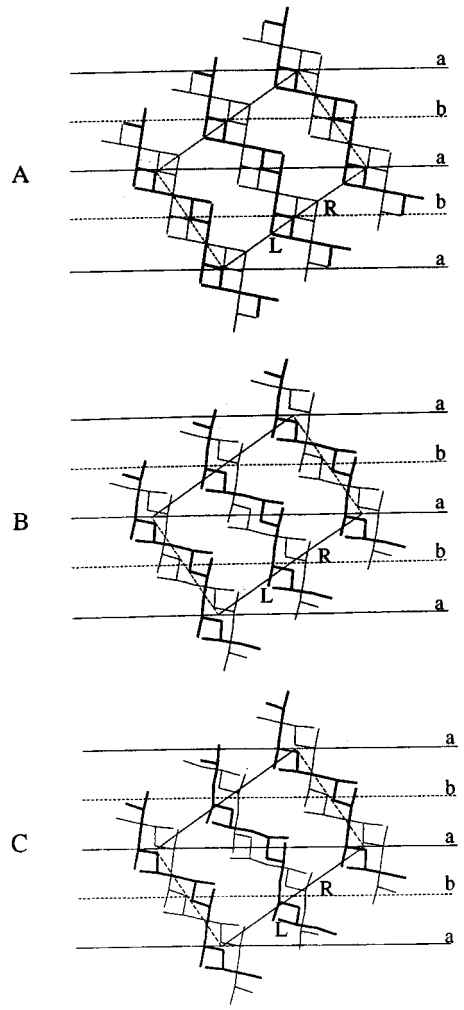

Figure 6. Unit cell projections with (011) planes on edge for the *Ibca* (A), *Pbca* (B), and $P2_1/a$ (C) space groups. The traces a, in phase, and b, out of phase, relative to the crystallographic (011) plane are indicated. R = right handed, L = left handed helix.

If the inversion centers which relate neighboring chains along the directions *x* and *y* are left, the space group becomes *B*2/*b* and the monoclinic unit cell has axes $a = 18.3$ Å, $b = 11.2$ Å (the same as the orthorhombic cell), and $c = 7.4$ Å and $\gamma = 127.7°$. The asymmetric unit corresponds as in *Pbca* to two monomeric units, the chains are free to rotate around their axes and to translate along *z*. The refinement of this model (space group *B*2/*b*) produces a convergence in the space group *Ibca* with a not satisfying agreement factor ($R_2' = 21\%$).

If the centering of the cell is removed, the symmetry left leads to $P2_1/b$ or $P2_1/a$ space groups (*c*, unique axis), if a unit cell nearly coincident with the old orthorhombic

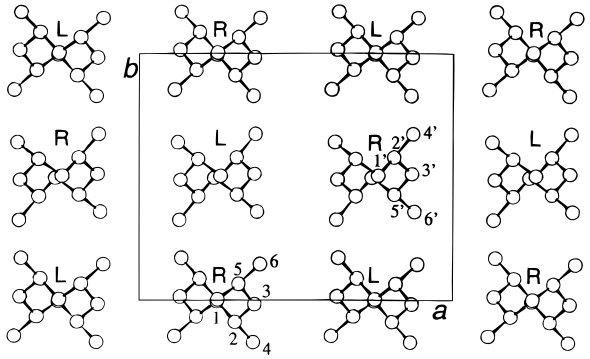

Figure 7. Refined packing model of form I of s-PP for the space group $P2_1/a$.

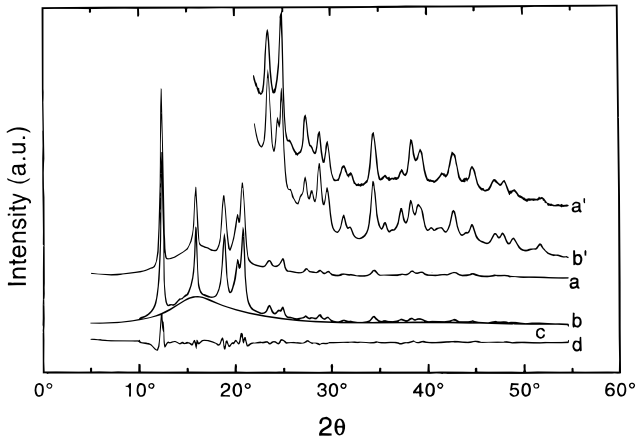

Figure 8. Comparison between the observed (curve a) and calculated, for the space group $P2_1/a$ (curve b), X-ray powder diffraction profiles of form I of s-PP. The X-ray profile of the amorphous sample suitably scaled (curve c) and the difference between observed and calculated profiles (curve d) are also shown. The experimental (curve a′) and calculated (curve b′) profiles for $2\theta > 22°$ on an enlarged intensity scale are also reported.

one is preserved. The asymmetric unit consists now of two independent chains with axes placed on the 2_1 symmetry elements, two monomeric units each, in both symmetries. The inversion centers may be left to relate the chains along the *b* axis (space group $P2_1/b$). In this case the model still converges to the *Ibca* space group (agreement factor $R_2' = 20\%$). Alternatively, the inversion centers relating the chains along the *a* axis are left (space group, $P2_1/a$). The refinement for this space group leads to a unit cell with axes $a = 14.31$ Å, $b = 11.15$ Å, and $c = 7.5$ Å and $\gamma = 90.3°$ (Figure 7) and produces an agreement factor $R_2' = 11.6\%$. A comparison between the observed (curves a and a′) and calculated for the space group $P2_1/a$ (curves b and b′) X-ray powder diffraction profiles is shown in Figure 8. It is apparent that the discrepancies which were still left for the space group *Pbca* are eliminated for the model of Figure 7 (space group $P2_1/a$).

The fractional coordinates of the asymmetric unit of the model of Figure 7 are reported in Table 1. The values of the refined structural and nonstructural parameters are reported in Tables 2 and 3, respectively. The calculated squared structure factors for the refined model are shown in Table 4.

In the refined model, the two independent chains are rotated in opposite directions: from the coordinates, as obtained, $\omega = 5.8°$ (unprimed chain in Figure 7) and $\omega = -4.4°$ (primed chain in Figure 7), as shown in Figure 9. Like in the *Pbca* space group, consecutive chains along the *b* axis are rotated around the chain axis by the same (or nearly the same) angle $|\omega|$ but in opposite directions, whereas consecutive chains along *a* are related by an inversion center and are rotated around the chain axis by the same amount, in the same direction. Figure 10 plots three first neighboring chains belonging to the same *bc* layer, whereas Figure 11 plots the packing situation among first neighboring helices belonging to consecutive *bc* layers along *a*. The *z*

Table 4. Calculated Squared Structure Factors ($F_c^2 = F^2M$, where *M* is the Multiplicity Factor) for the Model of Figure 7 of Form I of s-PP for the Space Group $P2_1/a$ and the Unit Cell with Axes $a = 14.31$ Å, $b = 11.15$ Å, $c = 7.5$ Å, and $\gamma = 90.3°$ [a]

hkl	d_{calc} (Å)	d_{obs} (Å)	F_c^2	hkl	d_{calc} (Å)	d_{obs} (Å)	F_c^2
200	7.155	7.21	2240	$\bar{3}32$	2.318		132
101	6.672		52	332	2.310		556
011	6.246		72	$\bar{3}41$	2.297	2.30	144
$\bar{1}11$	5.731		116	023	2.291		60
111	5.717	5.61	40	341	2.287		356
020	5.574		1658	042	2.241		136
$\bar{2}11$	4.713		2040	512	2.232		56
211	4.698	4.72	1512	$\bar{4}40$	2.204		118
021	4.482		488	440	2.193		58
$\bar{2}20$	4.409	4.41	812	223	2.180	2.18	92
220	4.385		888	313	2.179		88
$\bar{1}21$	4.283		2084	$\bar{2}42$	2.141		64
121	4.270	4.29	2784	$\bar{4}32$	2.132		32
301	4.031		48	432	2.124		512
$\bar{3}11$	3.797		252	$\bar{4}41$	2.116		44
221	3.790		52	$\bar{5}22$	2.113	2.12	328
311	3.786	3.80	272	151	2.113		44
002	3.770		324	522	2.107		128
102	3.645		528	441	2.105		72
400	3.579	3.59	708	$\bar{1}33$	2.061		148
012	3.570		48	403	2.057		36
112	3.464		148	$\bar{3}42$	2.032	2.03	440
202	3.335		104	342	2.025		208
031	3.333		40	602	2.016		44
$\bar{3}21$	3.274	3.27	392	$\bar{2}33$	2.001		32
321	3.260		32	612	1.982		44
212	3.193		344	$\bar{6}31$	1.944		52
022	3.122		172	532	1.940		152
$\bar{4}11$	3.109	3.11	268	631	1.935		32
411	3.101		448	$\bar{4}23$	1.931	1.93	316
$\bar{2}31$	3.027		332	423	1.927		92
$\bar{4}20$	3.019		44	541	1.925		36
231	3.016	3.02	108	$\bar{3}33$	1.910		96
420	3.004		146	$\bar{4}42$	1.903		412
$\bar{2}22$	2.865		164	$\bar{6}22$	1.899	1.90	72
312	2.857	2.86	220	442	1.895		108
$\bar{4}21$	2.803		128	104	1.869		60
421	2.790	2.80	44	043	1.866		232
$\bar{3}22$	2.617		636	$\bar{5}13$	1.863		76
322	2.609		248	513	1.861	1.86	132
$\bar{5}11$	2.605		68	060	1.858		82
$\bar{1}32$	2.604		220	143	1.850		100
$\bar{2}40$	2.601	2.61	34	451	1.831		56
132	2.600		88	$\bar{6}40$	1.817		34
511	2.600		64	243	1.804		72
240	2.592		34	702	1.798		72
141	2.569		32	800	1.789		84
412	2.525	2.54	312	352	1.777		48
232	2.479		116	$\bar{6}32$	1.775		56
$\bar{2}41$	2.451	2.47	56	$\bar{5}42$	1.768	1.77	264
521	2.418		480	632	1.768		180
$\bar{5}21$	2.408	2.41	204	542	1.761		64
$\bar{4}22$	2.357		604	304	1.753		156
422	2.349	2.36	356				

[a] Only reflections with $F_c^2 \geq 30$ are reported in the table. The Bragg distances observed in the powder spectrum (d_{obs}) are also reported.

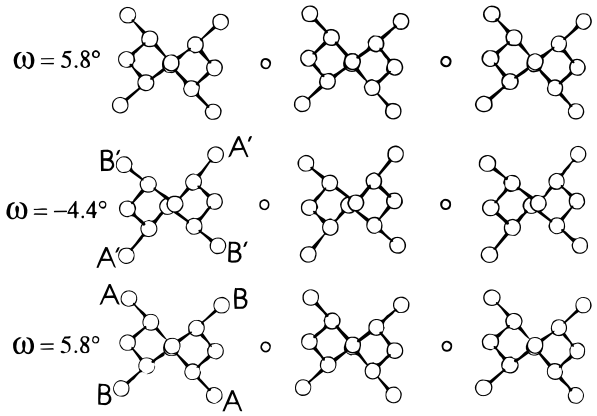

Figure 9. *a*−*b* projection of the refined packing model of s-PP in the $P2_1/a$ space group. Labels indicate crystallographically nonequivalent methyl groups. ω is the angle between an ideal axis perpendicular to the chain axis, crossing the CH_2 groups in a TG·GT conformational environment in the *a*−*b* projection and the *a* axis. R = right-handed, L = left-handed helix.

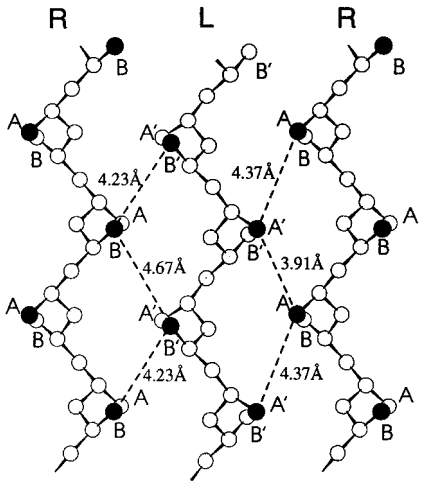

Figure 10. *b* sin γ−*c* projection of the refined packing model of s-PP in the $P2_1/a$ space group. The shortest distances between methyl carbon atoms of adjacent chains are shown.

coordinate of the methylene groups in a GT·TG conformational environment, C_1 and C_1', are displaced by $-0.032c$ and $0.112c$ along *z* from the height of the inversion centers at 0 of the $P2_1/a$ space group, respectively (see Table 1). In practice, in the refined models consecutive chains along *b* appear displaced by $\Delta z/c = 0.034$, on average, whereas couples of consecutive chains along *a* would be displaced by $\Delta z/c = 0.093$ in Figure 11a and by $\Delta z/c = 0.16$ in Figure 11b (the values of $\Delta z/c$ have been obtained by averaging over the *z*/*c* coordinates of the methyl carbon atoms). The average displacement between consecutive *bc* layers hence results $\approx 0.13c$ ($\approx$1 Å), similarly to the refined model in the *Pbca* space group. The shift pattern in the $P2_1/a$ space group is better visualized in Figure 6C, in the *bc* projection, as compared to the *Pbca* and *Ibca* space groups situations. The calculated intensity of the reflection at $d = 6.21$ Å ($2\vartheta = 14.25°$, Cu Kα, Miller indices (011)) in the refined $P2_1/a$ space group is not negligible (see Table 4) and is in reasonable agreement with the experimental intensity observed in the electron diffraction spectra.[8]

In the refined model $P2_1/a$ the contact distances between carbon atoms belonging to different chains are always higher than 3.9 Å. In Figures 10 and 11, only the contact distances between methyl carbon atoms are shown.

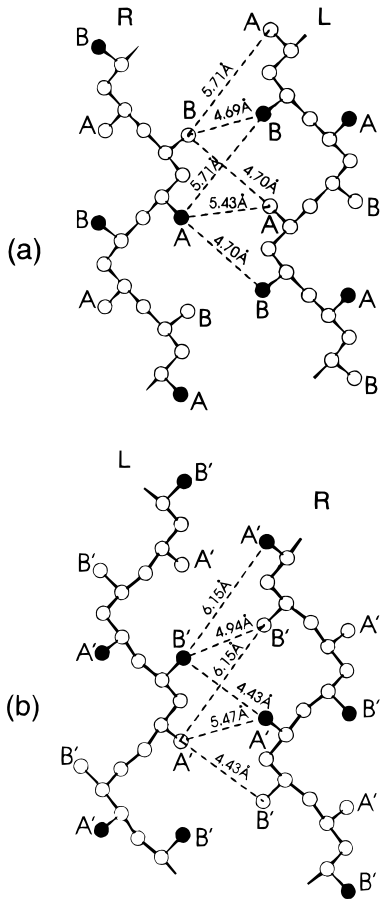

Figure 11. *a*−*c* projection of the refined packing model of s-PP in the $P2_1/a$ space group. The shortest distances between the methyl carbon atoms belonging to adjacent chains are shown. (a) and (b) correspond to different packing situations which arise between adjacent chains along *a* in the $P2_1/a$ space group.

Unlike the *Ibca* space group, implying that all the methyl groups were crystallographically equivalent, at least four different packing situations arise for the methyl groups in the refined model in the space group $P2_1/a$, as a consequence of the rotations around the chain axes and of the translations along *z* of the chains (see Figures 9−11). The four different methyl groups are indicated with the letters A, B, A′, and B′ in the figures. In the projection perpendicular to the *b* axis the chains are closely interdigitated[10] and the methyl groups A and A′ appear not equivalent, as far as the contacts with the nonbonded atoms, to the methyl groups B and B′ (see Figure 10). Methyl groups A (B) experience instead packing situations quite similar to those of methyl groups A′ (B′), as evidenced in Figure 11. This could explain the splitting of the resonance of the methyl carbons observed in the solid state ^{13}C NMR spectrum of the annealed form I of s-PP reported by Sozzani et al.[15]

Conclusion

The crystal structure of form I of s-PP has been analyzed in detail and a refinement of the structure has been performed with the Rietveld method.

The presence of the (011) reflection in the electron diffraction spectra of single crystals of s-PP grown at high temperatures[8] and the splitting of the resonance of the methyl carbons observed in the solid state ^{13}C NMR spectra of the annealed sample of s-PP,[15] showing an X-ray diffraction pattern typical of form I, indicate that the crystal structure of form I is described only

approximately by the space group *Ibca*. For this space group the (011) reflection is extinct and all the methyl carbons are equivalent.

Our refinement shows that a good agreement between experimental and calculated X-ray powder diffraction patterns is obtained with a mode of packing of the chains similar to that of the space group *Ibca* (i.e. chains of opposite chirality alternate along the *a* and *b* axes) but in a space group of lower symmetry. The crystal structure of form I is better described if the body centering of the unit cell is removed (the space group becomes *Pbca*). This results in a slight rotation of the chains around the chain axis of $\pm 5 \pm 1°$ and shifts of consecutive *bc* layers of macromolecules of $0.14c$ along the chain axis. However, the space group *Pbca* still implies the systematic extinction of the $0kl$ reflections with $k = 2n + 1$; the agreement with experimental data is improved by breaking the symmetry further on. For instance a monoclinic space group $P2_1/a$ is better suited to describe the crystal structure of form I. This implies a further shift, along *c*, of consecutive chains along *b* by $0.034c$. The unit cell is $a = 14.31 \pm 0.07$ Å, $b = 11.15 \pm 0.02$ Å, $c = 7.5 \pm 0.1$ Å, and $\gamma = 90.3 \pm 1.5°$. This model of packing explains the splitting of the resonance of the methyl carbons observed in the solid state ^{13}C NMR spectra of form I of s-PP.

Acknowledgments. We thank Dr. M. Galimberti of Montell for supplying the s-PP sample. Financial support from the Ministero dell' Università e della Ricerca Scientifica e Tecnologica is gratefully acknowledged.

References and Notes

(1) Natta, G.; Pasquon, P.; Zambelli, A. *J. Am. Chem. Soc.* **1962**, *84*, 1488.
(2) Zambelli, A.; Locatelli, P.; Rovasoli, A.; Ferro, D. R: *Macromolecules* **1980**, *13*, 267.
(3) Ammendola, P.; Shijing, X.; Grassi, A.; Zambelli, A. *Gazz. Chim. Ital.* **1988**, *118*, 769.
(4) Ewen, J. A.; Jones, R. J.; Razavi, A.; Ferrara, J. D. *J. Am. Chem. Soc.* **1988**, *110*, 6255.
(5) Lotz, B.; Lovinger, A. J.; Cais, R. E. *Macromolecules* **1988**, *21*, 2375.
(6) Lovinger, A. J.; Lotz, B.; Davis, P. D. *Polymer* **1990**, *31*, 2253.
(7) Lovinger, A. J.; Davis, D. D.; Lotz, B. *Macromolecules* **1991**, *24*, 552.
(8) Lovinger, A. J.; Lotz, B.; Davis, D. D.; Padden, F. J. *Macromolecules* **1993**, *26*, 3494.
(9) De Rosa, C.; Corradini, P. *Macromolecules* **1993**, *26*, 5711.
(10) Corradini, P.; Napolitano, R.; Pirozzi, B. *Rend. Fis. Acc. Lincei* **1991**, s. 9, *2*, 341.
(11) Auriemma, F.; De Rosa, C.; Corradini, P. *Macromolecules* **1993**, *26*, 5719.
(12) Auriemma, F.; De Rosa, C.; Corradini, P. *Rend. Fis. Acc. Lincei* **1993**, s. 9, *4*, 287.
(13) Balbontin, G.; Dainelli, D.; Galimberti, M.; Paganetto, G. *Makromol. Chem.* **1993**, *193*, 693.
(14) Sozzani, P.; Galimberti, M.; Balbontin, G. *Makromol. Chem., Rapid Commun.* **1993**, *13*, 305.
(15) Sozzani, P.; Simonutti, R.; Galimberti, M. *Macromolecules* **1993**, *26*, 5782.
(16) Chatani, Y.; Maruyama, H.; Noguchi, K.; Asanuma, T.; Shiomura, T. *J. Polym. Sci., Part C* **1990**, *28*, 393.
(17) Chatani, Y.; Maruyama, H.; Asanuma, T.; Shiomura, T. *J. Polym. Sci., Polym. Phys.* **1991**, *29*, 1649.
(18) Auriemma, F.; Born, R.; Spiess, H. W.; De Rosa, C.; Corradini, P. *Macromolecules* **1995**, *28*, 6902.
(19) Auriemma, F.; Lewis, R. H.; Spiess, H. W.; De Rosa, C. *Macromol. Chem. Phys.* **1995**, *196*, 4011.
(20) Natta, G.; Corradini, P.; Ganis, P. *Makromol. Chem.* **1960**, *39*, 238.
(21) Corradini, P.; Natta, G.; Ganis, P.; Temussi, P. A. *J. Polym. Sci., Part C* **1967**, *16*, 2477.
(22) Natta, G.; Peraldo, M.; Allegra, G. *Makromol. Chem.* **1964**, *75*, 215.
(23) Immirzi, A. *Acta Crystallogr.* **1980**, *B38*, 2378.
(24) Millini, R.; Perego, G.; Bruckner, S. *Mater. Sci. Forum* **1991** *71−82*, 239.
(25) Meille, S. V.; Bruckner, S.; Porzio, W. *Macromolecules* **1990**, *23*, 4114.
(26) Meille, S. V.; Ferro, D. R.; Bruckner, S. Lovinger, A. J.; Padden, J. *Macromolecules* **1994**, *27*, 2615.
(27) Trifuoggi, M.; De Rosa, C.; Auriemma, F.; Corradini, P.; Bruckner, S. *Macromolecules* **1994**, *27*, 3553.
(28) Tadokoro, H. *Structure of Crystalline Polymers*; John Wiley: New York, 1979.
(29) Allegra, G.; Bassi, I. W.; Meille, S. V. *Acta Crystallogr.* **1978**, *A34*, 652.
(30) Perego, G.; Cesari, M.; Allegra, G. *J. Appl. Crystallogr.* **1984**, *17*, 403.

MA9601326